Computer Methods in Applied Mechanics and Engineering 429 (2024) 117139

Contents lists available at ScienceDirect

Comput. Methods Appl. Mech. Engrg.

journal homepage: www.elsevier.com/locate/cma

Points of inflection of special eigenvalue functions as indicators of stiffness maxima/minima of proportionally loaded structures

A. Wagner [a,*], J. Kalliauer [a,b], M. Aminbaghai [a], H.A. Mang [a,c]

[a] Institute for Mechanics of Materials and Structures, TU Wien – Technische Universität Wien, Karlsplatz 13 - E202, 1040 Vienna, Austria
[b] Department of Civil and Environmental Engineering, MIT – Massachusetts Institute of Technology, 77 Massachusetts Avenue, Cambridge, 02139, MA, United States of America
[c] College of Civil Engineering, Tongji University, Siping Road 1239, Shanghai 200092, China

ARTICLE INFO

Keywords:
Maximum (minimum) stiffness
Finite element method
Linear eigenvalue problem
Indefinite coefficient matrices
Hybrid finite element
Points of inflection of eigenvalue curves

ABSTRACT

The stiffness of a proportionally loaded structure may continuously increase or decrease. As a special exception, it may be constant. On the other hand, an initially stiffening (softening) structure may turn into a softening (stiffening) structure. At the load level of such a change the stiffness of the structure attains an extreme value. The task of this work is to present mathematical conditions for these load levels. Lack of them represents a void in the pertinent literature. The practical significance of the aforementioned changes is the one of indicators of the mechanical behavior to be expected after their occurrence. The second and the last author have recently presented a condition for the load level at which the stiffness of a proportionally loaded structure becomes a minimum value. It is given as $d^2(\Re(\chi_1(\lambda)))/d\lambda^2 = 0$, representing the condition for a point of inflection of the real part of a complex eigenvalue function $\chi_1(\lambda)$, where λ denotes a dimensionless load parameter. The underlying linear eigenvalue problem has two indefinite coefficient matrices, which is a necessary condition for complex regions of eigenvalue functions. These matrices are established with hybrid elements, available in a commercial finite element program. In the present work, $d^2(\chi_1(\lambda))/d\lambda^2 = 0$ is shown to be the condition for the load level at which the stiffness of a proportionally loaded structure attains a maximum value. The eigenvalue function concerned has no complex region. It is also shown that the displacement elements, which are the basis for their extension to the employed hybrid elements, are unable to indicate the load level at an extreme value of the stiffness.

List of symbols

Nomenclature

Variable	Base	Explanation
e	L	Eccentricity of the normal force, illustrated in Fig. 2(a)
$\mathbf{f}$	various	Vector of nodal force degrees of freedom in the framework of the FEM, introduced in form of $d\mathbf{f}$ in (9)
k	M T^{-2}	Stiffness of a single d.o.f. member, introduced in (1)

* Corresponding author.
E-mail address: antonia.wagner@tuwien.ac.at (A. Wagner).

https://doi.org/10.1016/j.cma.2024.117139
Received 30 August 2023; Received in revised form 4 June 2024; Accepted 5 June 2024
Available online 28 June 2024

n	–	Number of displacement and force degrees of freedom in the FEM simulations, introduced in (5)
$\mathbf{r}$	various	Subvector of an eigenvector of the linear eigenvalue problem (4), associated with the nodal displacement degrees of freedom
$\mathbf{r}_1$	various	Subvector of the fundamental eigenvector of the linear eigenvalue problem (4), associated with the nodal displacement degrees of freedom, introduced in (6)
$\widehat{\mathbf{r}}$	various	Eigenvector of the linear eigenvalue problem (11)
$\mathbf{r}^\diamond$	various	Eigenvector of the linear eigenvalue problem (25)
$\mathbf{t}$	–	Subvector of an eigenvector of the linear eigenvalue problem (4), associated with the nodal force degrees of freedom
$\mathbf{t}_1$	–	Subvector of the fundamental eigenvector of the linear eigenvalue problem (4), associated with the nodal force degrees of freedom, introduced in (6)
$\mathbf{u}$	–; L	Vector of nodal displacement degrees of freedom in the framework of the FEM, introduced in form of $d\mathbf{u}$ in (9)
$\mathbf{u}^*$	L	Vector of nodal translational degrees of freedom, introduced in (31)
E	M L^{-1} T^{-2}	Modulus of elasticity
$\mathbf{G}$	various	Submatrix of one of the two coefficient matrices of the linear eigenvalue problem (4)
$\mathbf{G}_0$	various	$\mathbf{G}(\lambda = 0)$, introduced in (4)
I	–	Point of inflection, shown first in Fig. 1
I_1	–	Point of inflection of $\Re(\chi_1(\lambda))$, shown in Fig. 2(b)
I_j	–	Point of inflection of $\Re(\chi_j(\lambda))$, shown in Fig. 2(b)
$\mathbf{K}$	various	Tangent stiffness matrix, representing a submatrix of one of the two coefficient matrices of the linear eigenvalue problem (4)
$\mathbf{K}_0$	various	$\mathbf{K}(\lambda = 0)$, introduced in (4)
$\widehat{\mathbf{K}}$	various	Tangent stiffness matrix, representing one of the two coefficient matrices of the linear eigenvalue problem (11)
$\widehat{\mathbf{K}}_0$	various	$\widehat{\mathbf{K}}(\lambda = 0)$, introduced in (11)
L	L	Length of a bar, introduced in Fig. 2(a)
P	M L T^{-2}	Force acting on a single d.o.f. member, introduced in (1)
$\overline{P}$	M L T^{-2}	Reference load, shown first in Fig. 2(a)
$\overline{\mathbf{P}}$	M L T^{-2} ; M L^2 T^{-2}	Vector of reference work-equivalent node forces, introduced in (9)
$\overline{\widehat{\mathbf{P}}}$	M L T^{-2}	Vector of reference work-equivalent node forces, introduced in (8)
R	L	Radius of a circular arch, shown in Fig. 4
S	–	Stability limit, shown first in Fig. 3(a)
U	M L^2 T^{-2}	Strain energy, introduced in (22)
$U_{\mathbf{M}}$	M L^2 T^{-2}	Contribution of bending and torsion to U, introduced in (22)
s	L	Axial coordinate, introduced in form of ds in (30)
u	L	Deformation of a single d.o.f. member, introduced in Fig. 1; tangential displacement, introduced in Fig. 6
u_{ave}	L	Average displacement, defined in (31)
x	L	Component of the co-ordinate system, shown in Figs. 2, 4, and 5
y	L	Component of the co-ordinate system, shown in Figs. 2, 4, and 5
κ	–	Shear coefficient, introduced in Fig. 4
λ	–	Proportionality factor of reference forces, shown in Figs. 2–4 and 6 and 8
λ_L	–	Lower bound of the complex region of χ_1 and $\chi_j = \overline{\chi}_1$, shown in Fig. 2(b)
λ_S	–	Value of λ at the stability limit S, shown first in Fig. 3(a).
λ_U	–	Upper bound of the complex region of χ_1 and $\chi_j = \overline{\chi}_1$, shown in Fig. 2(b)
μ	–	Read angle of a circular arch, shown in Fig. 4
ν	–	Poisson's ratio
ξ	–	Arc length of the FEM-displacements, defined in (30)
ϕ	–	Rotation of the tangent, illustrated in Fig. 6
χ	–	Eigenvalue of the linear eigenvalue problem (4)
χ_1	–	Fundamental eigenvalue of the linear eigenvalue problem (3), shown first in Fig. 2(b)
$\overline{\chi}_1$	–	$\overline{\chi}_1 = \chi_j$, fundamental conjugate complex eigenvalue in the complex region of χ_1 and χ_j; χ_1 is shown in Fig. 2(b)
$\widehat{\chi}$	–	Eigenvalue of the linear eigenvalue problem (11)

$\chi^{\diamond}$	–	Eigenvalue of the linear eigenvalue problem (25)
$\Re(\chi_1(\lambda))$	–	Real part of the complex eigenvalue χ_1 and of the conjugate complex eigenvalue $\chi_j = \overline{\chi}_1$, introduced in the description of Fig. 2(b)

1. Introduction

Stiffness is a key term of structural mechanics. It either refers to materials or, as is the case in this work, to structures. The stiffness of a proportionally loaded structure may continuously increase or decrease. As a special exception it may be constant. On the other hand, an initially stiffening (softening) structure may turn into a softening (stiffening) structure. At the load level of such a change, the stiffness of the structure attains an extreme value. There is no generally accepted mechanical definition of the stiffness of structures that represent multi degree-of-freedom (d.o.f.) systems. (*Per se*, the term *stiffness* of such structures is less significant than the qualitative terms *stiffening* and *softening*, which signal important trends of structural behavior.) However, the term *stiffness* is well defined for structural members that are single d.o.f. systems. Fig. 1(a) (Fig. 1(b)) shows a load–displacement diagram of such a structural member. It contains a point of inflection, denoted as I. This point defines the load, $P = P_I$, and the corresponding deformation, $u = u_I$, for which the stiffness of the structural member becomes an extreme value. With

$$k = \frac{dP}{du} > 0 \tag{1}$$

as the definition of the stiffness, k, point I is characterized by

$$\frac{dk}{du} = \frac{d^2P}{du^2} = 0. \tag{2}$$

This point defines the transition from a stiffening (softening) to a softening (stiffening) single d.o.f.system. (It is worth mention that the meaning of the term *softening* in material mechanics differs from the one used herein.)

The goal of this work is to present mathematical conditions for the load level at extreme values of the stiffness of multi d.o.f. systems, *i.e.* of structures, subjected to a proportionally increasing load. In general, load–displacement diagrams of individual d.o.f.s differ considerably. Moreover, in the framework of the Finite Element Method (FEM), which will be used to achieve the aforementioned goal, the individual d.o.f.s have, in general, different physical dimensions. Hence, it is usually impossible to determine the load level at which an extreme value of the stiffness of a structure occurs on the basis of selected d.o.f.s and, the less, by a single d.o.f.

From the viewpoint of fundamental research in structural mechanics the significance of extreme values of the stiffness of proportionally loaded structures is undisputed. Their practical significance is the one of indicators of the mechanical behavior to be expected after the transition from a stiffening (softening) to a softening (stiffening) structure. The rationale behind the former is that the decrease of the stiffness of the structure after this transition will, in general, lead to buckling. The rationale behind the latter is that the increase of the stiffness of the structure after the respective transition temporarily postpones the structure's tendency towards loss of stability. The difference between the comment on stiffness maxima and the one on stiffness minima insinuates a fundamental mechanical difference between the two kinds of extreme values, entailing fundamentally different mathematical conditions. In this context it deserves mention that buckling is *per se* not restricted to softening structures [1]. In other words, also structures with continuously increasing stiffness may buckle.

In view of the global nature of extreme values of the stiffness of proportionally loaded structures, linear eigenvalue analysis, in the framework of the FEM, is the proper means to the end of finding mathematical conditions for the load level at extreme values of the stiffness of proportionally loaded structures. A first attempt in this direction by Kalliauer and Mang [2] has led to a condition for minimum stiffness of such structures. By coincidence, a linear eigenvalue problem, originally proposed by Malendowski in [3], has

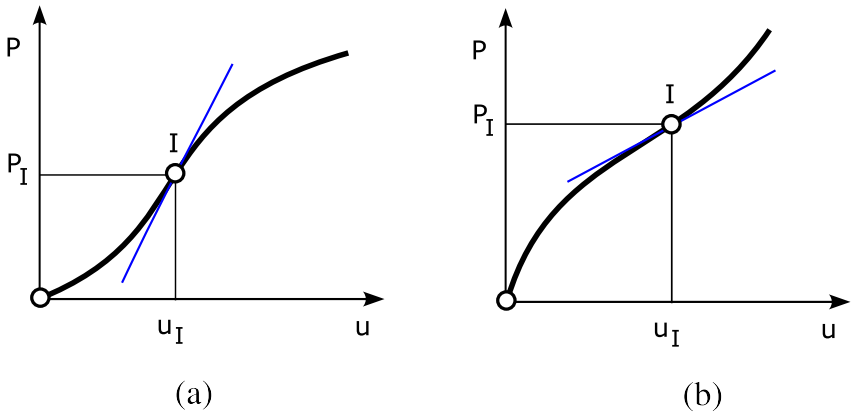

Fig. 1. Single d.o.f. systems with (a) maximum stiffness and (b) minimum stiffness, at point I.

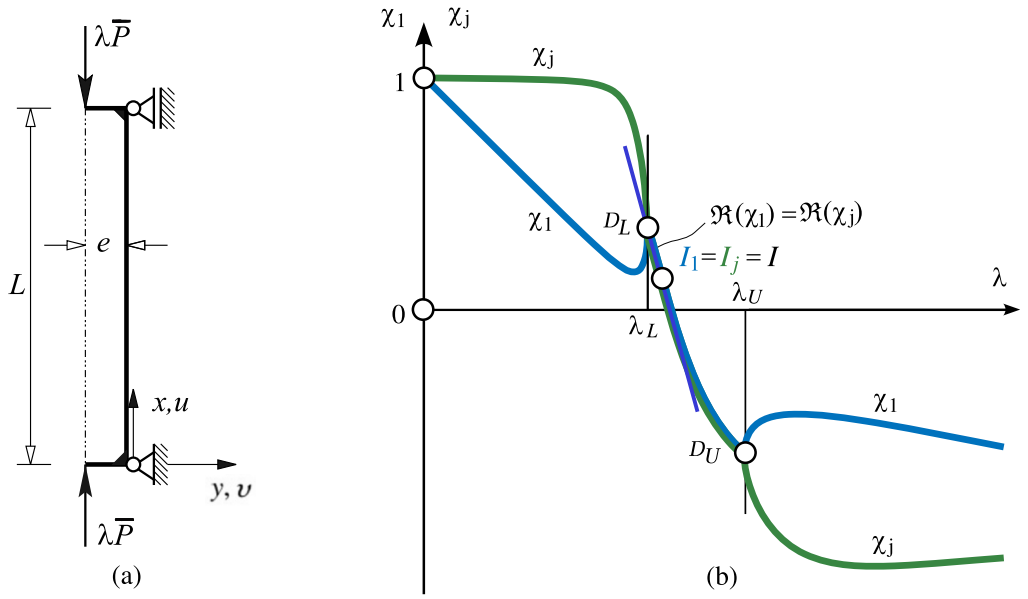

Fig. 2. Bar subjected to an eccentric compressive force: (a) undeformed structure, (b) $\chi_1(\lambda)$ and $\chi_j(\lambda)$ for $0 \le \lambda \le \lambda_L$ and $\lambda \ge \lambda_U$, $\Re(\chi_1(\lambda)) = \Re(\chi_j(\lambda))$ for $\lambda_L < \lambda < \lambda_U$.

turned out to be the proper tool for finding this condition. To give a brief explanation of the nature of this serendipity-like finding, the key result of the numerical example in [2] will be reproduced in the following. Its purpose is to facilitate the introduction to the topic of this paper without the need of delving into [2]. At the time when the initially surprising result for the load level at minimum stiffness of a proportionally loaded structure was obtained, the authors had no hint about the kind of duality of the conditions for stiffness maxima and minima.

Fig. 2(a) shows a simply supported bar subjected to eccentric compression. Geometric details and material parameters are given in [2]. Fig. 2(b) illustrates two eigenvalue curves, $\chi_1(\lambda)$ and $\chi_j(\lambda)$, where λ denotes a dimensionless load parameter. The underlying linear eigenvalue problem [2], which will the discussed in detail in Section 2, enables eigenvalue functions to become complex functions inside finite regions of λ. In the interval $(\lambda_L,\ \lambda_U)$ in Fig. 2(b), $\Re(\chi_1) = \Re(\chi_j)$, where the symbol $\Re$ stands for *real part*, and where $\chi_j = \overline{\chi}_1$ is the conjugate complex eigenvalue of χ_1. In [2] it was shown that the value of λ at the point of inflection, $I_1 = I_j = I$, of this curve is the load level at which the stiffness of the bar attains a minimum value. With the exception of this point, the two eigenvalue functions $\chi_1(\lambda)$ and $\chi_j(\lambda)$ are mechanically insignificant. *Nota bene,* unless the expression for the curvature of the bar is linearized, a stability limit does not exist in case of a linear elastic material. This is reflected by the fact that it is just the real part of $\chi_1(\lambda)$ and $\chi_j(\lambda)$ that intersects the λ-axis in Fig. 2(b). While $\Re(\chi_1) = \Re(\chi_j) = 0$ has no physical meaning, the vanishing of a real fundamental eigenvalue function, *i.e.* $\chi_1 = 0$, is the buckling condition, as will be shown in Section 2. A necessary condition for complex eigenvalues of a linear eigenvalue problem is that both coefficient matrices are indefinite matrices [4]. However, it needs a physical reason for a part of $\chi_1(\lambda)$ to become a complex function. In the given case it is the existence of a minimum value of the stiffness of the bar in the interval $\left[\lambda_L,\ \lambda_U\right]$, see Fig. 2(b). Inside this interval, loss of stability is impossible. However, the existence of a minimum value of the stiffness cannot preclude the possibility of buckling at a higher load level. This explains the return of the two conjugate complex eigenvalues χ_1 and χ_j to real eigenvalues at $\lambda = \lambda_U$.

The opposite of escaping buckling by a transition from softening to stiffening in case of proportional loading of structures is loss of stability preceded by the transition from stiffening to softening. For a single d.o.f. system, as shown in Fig. 1(a), this transition is characterized by $d^2P/du^2 = 0$ and $d^3P/du^3 < 0$. As will be shown in this work, the corresponding conditions for multi d.o.f. systems read as $d^2\chi_1/d\lambda^2 = 0$ and $d^3\chi_1/d\lambda^3 < 0$. For a single d.o.f. system, as shown in Fig. 1(b), the transition from softening to stiffening is characterized by $d^2P/du^2 = 0$ and $d^3P/du^3 > 0$. The corresponding conditions for multi d.o.f. systems, reported in [2], read as $d^2(\Re(\chi_1))/d\lambda^2 = 0$ and $d^3(\Re(\chi_1))/d\lambda^3 > 0$.

Conditions for extreme values of the stiffness of structures are considered as fundamental ingredients of structural mechanics. Lack of such conditions is viewed as a void of the literature in this scientific field. The purpose of the present paper is to fill this void.

To the best knowledge of the authors, literature by other research groups on conditions for extreme values of the stiffness of proportionally loaded structures in the framework of computational mechanics does not seem to exist. This explains the sparseness of literature cited in this paper.

The remaining part of this work is organized as follows: Section 2 is devoted to the linear eigenvalue problem serving as the tool for determination of mathematical conditions for extreme values of proportionally loaded structures. This eigenvalue problem is a vehicle for so-called *accompanying linear eigenvalue analysis*. In the early days of structural stability analysis by the FEM this

mode of analysis served the purpose of circumventing numerical problems in the vicinity of the stability limit. With the exception of the zero position of the eigenvalue function $\chi_1(\lambda)$ at the stability limit, this function is *per se* mechanically insignificant. In the present research, the limited mechanical significance of $\chi_1(\lambda)$ is extended to points of inflection of $\chi_1(\lambda)$ and $\Re(\chi_1(\lambda))$, signaling stiffness maxima and minima, respectively. Section 3 deals with hybrid finite elements, required for determination of the two real, symmetric, indefinite coefficient matrices of this eigenvalue problem, allowing for conjugate complex eigenvalues. Section 4 contains the numerical investigation. It deals with a segment of a circular arch, clamped at one end and hinged at the other one [5]. The structure is subjected to a vertical point load, acting at its apex. Characteristic features of the structural behavior of this arch are the anticipated existence of a maximum value of its stiffness, followed by a maximum value of the percentage bending energy of the total strain energy before loss of stability by snap-through [6]. The reason for the restriction of the numerical investigation to linear elasticity is to show that extreme values of the stiffness of proportionally loaded structures may occur even for the simplest possible form of material behavior. The last section contains the conclusions drawn from the present research and an outlook on its potential extension.

2. Linear eigenvalue problem

The conditions for a minimum value of the stiffness of proportionally loaded structures, originally reported in [2], were given in the Introduction. They involve the real part of a complex eigenvalue. A necessary condition for complex eigenvalues is the indefiniteness of both coefficient matrices of the underlying linear eigenvalue problem [4]. Since it is not a sufficient condition, complex fundamental eigenvalues will not occur in the absence of a stiffness minimum, *i.e.* without a mechanical reason. The two $(n \times n)$ matrices can formally be written as

$$\left[\begin{array}{c|c} \mathbf{K} & \mathbf{G}^T \\ \hline \mathbf{G} & \mathbf{0} \end{array}\right] \quad \wedge \quad \left[\begin{array}{c|c} \mathbf{K}_0 & \mathbf{G}_0^T \\ \hline \mathbf{G}_0 & \mathbf{0} \end{array}\right]. \tag{3}$$

The submatrix $\mathbf{K} = \mathbf{K}(\lambda)$ in (1) denotes the $(m \times m)$ tangent stiffness matrix in the framework of the FEM, whereas the submatrix $\mathbf{K}_0 = \mathbf{K}(\lambda = 0)$ stands for the small-displacement stiffness matrix. The existence of the two $((n-m) \times m)$ submatrices $\mathbf{G}(\lambda)$ and $\mathbf{G}_0 = \mathbf{G}(\lambda = 0)$ makes complex eigenvalues possible. This allows to distinguish between the condition for minimum stiffness and the one for maximum stiffness. In contrast to the latter, the former is associated with a complex eigenvalue. $\mathbf{G}^T$ and $\mathbf{G}_0^T$ denote the transpose of $\mathbf{G}$ and $\mathbf{G}_0$, respectively. Both coefficient matrices are symmetric. They are the consequence of the assemblage of extended element tangent stiffness matrices. The reason for these local extensions is purely numerical, as will be explained in Chapter 3. It has nothing to do with the present research. In the prebuckling region, $\mathbf{K}(\lambda)$ is a positive-definite matrix. Hence, $\mathbf{K}_0$ is a positive-definite matrix. The two above coefficient matrices, however, are indefinite matrices, since they do not satisfy the conditions for definite matrices, according to which, *e.g.* for a positive-definite matrix, all principal minors must be positive [4].

The linear eigenvalue problem, containing the two coefficient matrices (3), can formally be written as

$$\left[\begin{array}{c|c} \mathbf{K} - \chi\mathbf{K}_0 & \mathbf{G}^T - \chi\mathbf{G}_0^T \\ \hline \mathbf{G} - \chi\mathbf{G}_0 & \mathbf{0} \end{array}\right] \cdot \left\{\begin{array}{c} \mathbf{r} \\ \hline \mathbf{t} \end{array}\right\} = \left\{\begin{array}{c} \mathbf{0} \\ \hline \mathbf{0} \end{array}\right\}, \tag{4}$$

where χ denotes an eigenvalue and $\lfloor \mathbf{r}^T, \mathbf{t}^T \rfloor$ stands for the corresponding eigenvector, consisting of the two subvectors $\mathbf{r}$ and $\mathbf{t}$; mathematically, the components of $\mathbf{t}$ represent Lagrange multipliers. The components of $\mathbf{r}$ and $\mathbf{t}$ have different physical dimensions. Without modifications, reference to which will be made in this Subchapter, they are mechanically insignificant. Specialization of (4) for $\lambda = 0$ gives

$$\chi_i = 1, \qquad i = \{1, 2, \dots, n\}, \tag{5}$$

representing an n–fold eigenvalue. Specialization of (4) for a stability limit, $\lambda = \lambda_S$, yields

$$\mathbf{K} \cdot \mathbf{r}_1 = \mathbf{0}, \quad \chi = \chi_1 = 0, \quad \mathbf{G} \cdot \mathbf{r}_1 = \mathbf{0}, \quad \mathbf{G}^T \cdot \mathbf{t}_1 = \mathbf{0}, \tag{6}$$

noting that, for $\lambda = \lambda_S$, $\mathbf{K}$ is a positive-semidefinite matrix that is singular [4]. χ_1 is termed as the fundamental eigenvalue; $\mathbf{r}_1$ and $\mathbf{t}_1$ represent the two subvectors of the respective eigenvector.

One of two reasons for the choice of the second coefficient matrix is its constancy. The other one is the equality of the physical dimension of corresponding coefficients of the two matrices in (3). This enables to make the characteristic polynomial of (4) dimensionless [2]. As mentioned previously, the components of the $(m \times 1)$ subvector $\mathbf{r}$ and of the $((n-m) \times 1)$ subvector $\mathbf{t}$ of the eigenvector have different physical dimensions. This is irrelevant to the present work insofar as eigenvectors are not needed. However, to stress the necessity of using a linear eigenvalue problem of the kind of (4) in this research, a comment on the correlation of $\ddot{\chi}_1 = 0$ $((\Re(\chi_1))^{\cdot\cdot} = 0)$ for maximum (minimum) stiffness on the "eigenvalue level" with its counterpart on the "eigenvector level" is deemed useful. This counterpart is assumed to be $\ddot{s} = 0$, where s denotes the arc-length of a curve on the surface of a unit hypersphere in the n-dimensional Euclidean space.

Beginning with the correlation of $\ddot{\chi}_1 = 0$ and $\ddot{s}_1 = 0$, the mentioned curve is described by the vertex of a vector $\tilde{\mathbf{r}}$ of length 1. $\|\dot{\tilde{\mathbf{r}}}\| = \dot{s}$ denotes the speed of the vertex of $\tilde{\mathbf{r}}$. This vector is a modification of the eigenvector $\lfloor \mathbf{r}^T, \mathbf{t}^T \rfloor$ of the linear eigenvalue problem (4). It serves the purpose of converting the components of the eigenvector, which have different physical dimensions, to dimensionless quantities. This is required for computation of the Euclidean norm, $\|\tilde{\mathbf{r}}\| = 1$, needed for determination of $\dot{s}$. For

example, for an eigenvector with three d.o.f.s, r_1, r_2, t_1, the components of $\tilde{\mathbf{r}}$ are given as $\sqrt{k_{11}^{(0)}}r_1, \sqrt{k_{22}^{(0)}}r_2, (g_{11}^{(0)}/\sqrt{k_{11}^{(0)}})t_1$, resulting in

$$\|\tilde{\mathbf{r}}\|^2 = k_{11}^{(0)}r_1^2 + k_{22}^{(0)}r_2^2 + \frac{(g_{11}^{(0)})^2}{k_{11}^{(0)}}t_1^2 = 1. \tag{7}$$

The constant, positive factors $k_{11}^{(0)}$, $k_{22}^{(0)}$ and $(g_{11}^{(0)})^2/k_{11}^{(0)}$ in (7) follow from the second matrix in (3), which refers to the onset of loading. In Appendix A of [2], the dimensions of $k_{11}^{(0)}$, $k_{22}^{(0)}$, and $g_{11}^{(0)}$ were chosen as [M T^{-2}], [M L^{2}T^{-2}], and [M$^{(1/2)}$T^{-1}], where M, L, and T stand for mass, length, and time, respectively. This enables determination of the dimensions of r_1, r_2, and t_1. In this context it is re-emphasized that (a) eigenvectors are irrelevant to the present work and that (b) they are *per se* mechanically insignificant.

Hence, a maximum value of the stiffness of a proportionally loaded structure correlates with an extreme value of the speed of the vertex of the unit vector $\tilde{\mathbf{r}}$, *i.e.* with $\ddot{s} = 0$. It is this correlation that distinguishes $\ddot{s} = 0$ from points of inflection of $s(\lambda)$ that do not correlate with $\ddot{\chi}_1 = 0$. Such unphysical points of inflection would be obtained if the fundamental eigenvectors were either left unaltered or if they were altered incorrectly. The described correlation between points of inflection on the "eigenvalue level" with points of inflection on the "eigenvector level" is formally analogous to the well-known correlation at loss of stability, see (6). For a long time, efficient determination of bifurcation points and snap-through points has been an important topic of research in the area of computational stability analysis of structures. As an example, a general procedure for the direct computation of these points [7] is mentioned. Ongoing research aims at proving that a maximum (minimum) value of $\dot{s}$, characterized by $\ddot{s} = 0$ and $\dddot{s} < 0$ (> 0), correlates with $(U_{\mathbf{M}}/U)^{\cdot} > 0$ (< 0), where U denotes the strain energy of the structure at the load level concerned and $U_{\mathbf{M}}$ stands for the part of U, resulting from bending, torsion, and shear.

Analogous to the correlation of $\ddot{\chi}_1 = 0$ with $\|\dot{\tilde{\mathbf{r}}}\|^{\cdot} = \ddot{s} = 0$, $(\mathfrak{R}(\chi_1))^{\cdot\cdot} = 0$ correlates with $\|(\mathfrak{R}(\tilde{\mathbf{r}}))^{\cdot}\|^{\cdot} = \ddot{s} = 0$. Again, $\ddot{s} = 0$ and $\dddot{s} < 0$ (> 0) is assumed to correlate with $(U_{\mathbf{M}}/U)^{\cdot} > 0$ (< 0).

The described correlations between points of inflection on the "eigenvalue level" with points of inflection, albeit of another kind, on the "eigenvector level" are a benefit of the parameterization with the load parameter λ. If, instead of it, the arc-length were chosen as the parameter, the speed of the vertices of the modified eigenvectors would be constant and equal to 1 [4]. Hence, points of inflection on the "eigenvector level" would not exist.

Apart from the subsidiary conditions $(\mathbf{G} - \chi\mathbf{G}_0)\cdot\mathbf{r} = \mathbf{0}$, (4) belongs to a category of linear eigenvalue problems that have played a great role in the early days of structural stability analysis by the FEM. These eigenvalue problems were the tool of so-called *accompanying linear eigenvalue analysis* [8]. The underlying linear eigenvalue problem has the general form $\left[\check{\mathbf{K}} - \check{\chi}\,\mathbf{B}\right]\cdot\check{\mathbf{r}} = \mathbf{0}$, where $\check{\mathbf{K}}$ denotes the tangent stiffness matrix [9]. Because of $\left|\check{\mathbf{K}}(\lambda_S)\right| = 0 \Leftrightarrow \check{\chi}_1(\lambda_S) = 0$, the real, symmetric coefficient matrix $\mathbf{B}$ of this eigenvalue problem has no influence on λ_S. With the exception of the vanishing of $\check{\chi}_1(\lambda_S)$, the solution of this linear eigenvalue problem has no mechanical significance. This explains the irrelevance of the choice of different submatrices $\mathbf{B}$ by different authors, see *e.g.* [8,10,11]. For the given problem, however, the fundamental eigenvalue of (4), $\chi_1(\lambda)$, is a tool for determination of the value of λ, for which an extreme value of the stiffness of a proportionally loaded structure is assumed to occur in the prebuckling region [2]. Hence, the selection of the two coefficient matrices of the underlying linear eigenvalue problem is not left to one's discretion. This explains the rather unconventional form of the underlying linear eigenvalue problem (4).

3. Finite elements

The eigenvector of the linear eigenvalue problem (4) consists of the two subvectors $\mathbf{r}$ and $\mathbf{t}$. Hence, it requires hybrid finite elements for determination of the element matrices which are then assembled to the two matrices (3) of this eigenvalue problem. In the given case, these elements are quadratic 3D Timoshenko-beam elements B32H and B32OSH, available in the element library of the commercial FE program Abaqus [12]. (The letter symbols B, H, and OS stand for *b*eam, *h*ybrid, and *o*pen cross-*s*ections, respectively. The numbers 3 and 2 refer to the terms *3D space and quadratic Timoshenko ansatz functions*, respectively.) These elements are extensions of the Abaqus displacement elements B32 and B32OS, respectively [12]. The equilibrium equations obtained with the latter for an infinitesimal increment of work-equivalent node forces, $d\lambda\overline{\widehat{\mathbf{P}}}$, where $\overline{\widehat{\mathbf{P}}}$ denotes the vector of reference node forces, can formally be written as

$$\widehat{\mathbf{K}}\cdot d\widehat{\mathbf{u}} = d\lambda\overline{\widehat{\mathbf{P}}}, \tag{8}$$

where $\widehat{\mathbf{K}}$ denotes the tangent stiffness matrix, obtained with the displacement elements B32 and B32OS, respectively, and $d\widehat{\mathbf{u}}$ stands for an infinitesimal increment of the vector of nodal displacements. The extended equilibrium equations for an infinitesimal increment of work-equivalent node forces $d\lambda\overline{\mathbf{P}}$, where $\overline{\mathbf{P}}$ denotes the vector of reference node forces, can formally be written as

$$\left[\begin{array}{c|c} \mathbf{K} & \mathbf{G}^T \\ \hline \mathbf{G} & \mathbf{0} \end{array}\right]\cdot\left\{\begin{array}{c} d\mathbf{u} \\ \hline d\mathbf{f} \end{array}\right\} = d\lambda\left\{\begin{array}{c} \overline{\mathbf{P}} \\ \hline \mathbf{0} \end{array}\right\}, \tag{9}$$

where $d\mathbf{u}$ and $d\mathbf{f}$ denote infinitesimal increments of the displacement and force d.o.f.s, respectively. The matrix on the left-hand side of (9), which is equal to one of the two coefficient matrices of the linear eigenvalue problem (4), is an assemblage of extended element tangent stiffness matrices. The respective extension on the element level manifests itself in the inclusion of $\mathbf{G}$ and $\mathbf{G}^T$ on the global level. The displacement nodal d.o.f.s of the hybrid elements are the same as the d.o.f.s of the displacement elements. Thus, disregarding discretization errors,

$$\mathbf{u} = \hat{\mathbf{u}}. \tag{10}$$

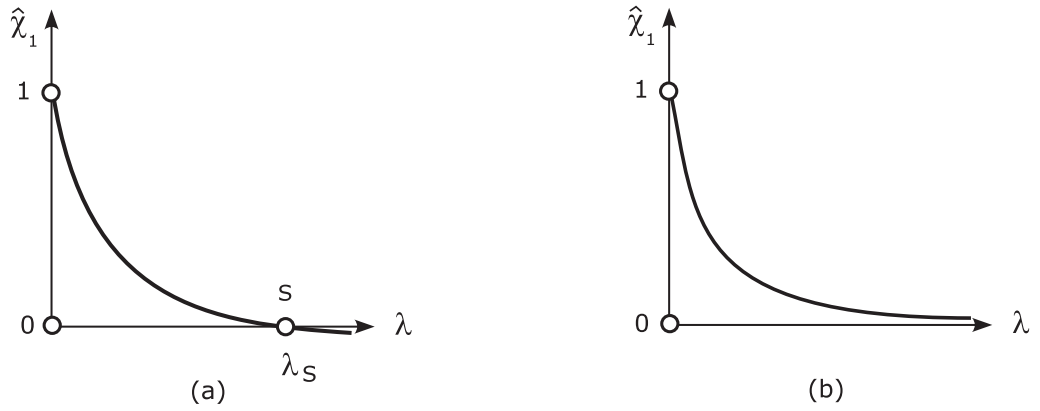

Fig. 3. Diagrammatic sketches of the fundamental eigenvalue $\hat{\chi}_1(\lambda)$, inspired by numerical results obtained with the Abaqus displacement beam element B32OS for a problem (a) with and (b) without a stability limit, see [2].

This raises the question for the motivation of the extension of the displacement elements to hybrid elements. The answer to this question is to avoid numerical problems with the displacement elements in case of nearly incompressible material [12]. The mathematical starting point of the said extension is a variational principle with subsidiary conditions [12]. They are the basis of the subsidiary conditions for the subvector $\mathbf{r}$ of the eigenvector $\lfloor \mathbf{r}^T, \mathbf{t}^T \rfloor^T$ in the underlying linear eigenvalue problem (4). Analogous to the formal correlation of (4) and (9), (8) formally correlates with the linear eigenvalue problem

$$\left[\hat{\mathbf{K}} - \hat{\chi}\,\hat{\mathbf{K}}_0\right] \cdot \hat{\mathbf{r}} = \mathbf{0}, \tag{11}$$

where $\hat{\mathbf{K}}_0 = \hat{\mathbf{K}}(\lambda = 0)$ and $\hat{\chi}(\lambda_S) = \chi(\lambda_S) = 0$. In (11), $\hat{\chi}$ denotes an eigenvalue and $\hat{\mathbf{r}}$ stands for the corresponding eigenvector. Contrary to the linear eigenvalue problem (4), the linear eigenvalue problem (11) does not contain two indefinite coefficient matrices.

In order to elucidate the necessity of using hybrid elements for the present research, typical fundamental eigenvalue functions χ_1 and $\hat{\chi}_1$ will be compared in the following. For this purpose, the mathematical formulations of the linear eigenvalue problems (4) and (11) are differentiated with respect to λ. This gives

$$\left[\begin{array}{c|c} \dot{\mathbf{K}} - \dot{\chi}\mathbf{K}_0 & \dot{\mathbf{G}}^T - \dot{\chi}\mathbf{G}_0^T \\ \hline \dot{\mathbf{G}} - \dot{\chi}\mathbf{G}_0 & \mathbf{0} \end{array}\right] \cdot \left\{\begin{array}{c} \mathbf{r} \\ \hline \mathbf{t} \end{array}\right\} + \left[\begin{array}{c|c} \mathbf{K} - \chi\mathbf{K}_0 & \mathbf{G}^T - \chi\mathbf{G}_0^T \\ \hline \mathbf{G} - \chi\mathbf{G}_0 & \mathbf{0} \end{array}\right] \cdot \left\{\begin{array}{c} \dot{\mathbf{r}} \\ \hline \dot{\mathbf{t}} \end{array}\right\} = \left\{\begin{array}{c} \mathbf{0} \\ \hline \mathbf{0} \end{array}\right\}, \tag{12}$$

and

$$\left[\dot{\hat{\mathbf{K}}} - \dot{\hat{\chi}}\hat{\mathbf{K}}_0\right] \cdot \hat{\mathbf{r}} + \left[\hat{\mathbf{K}} - \hat{\chi}\hat{\mathbf{K}}_0\right] \cdot \dot{\hat{\mathbf{r}}} = \mathbf{0}, \tag{13}$$

respectively. Then, (12) is premultiplied by $\lfloor \mathbf{r}^T, \mathbf{t}^T \rfloor$. Consideration of (4) results in

$$\dot{\chi} = \frac{\mathbf{r}^T \cdot \dot{\mathbf{K}} \cdot \mathbf{r} + 2\,\mathbf{t}^T \cdot \dot{\mathbf{G}} \cdot \mathbf{r}}{\mathbf{r}^T \cdot \mathbf{K}_0 \cdot \mathbf{r} + 2\,\mathbf{t}^T \cdot \mathbf{G}_0 \cdot \mathbf{r}}. \tag{14}$$

Analogously, (13) is premultiplied by $\hat{\mathbf{r}}^T$. Consideration of (11) results in

$$\dot{\hat{\chi}} = \frac{\hat{\mathbf{r}}^T \cdot \dot{\hat{\mathbf{K}}} \cdot \hat{\mathbf{r}}}{\hat{\mathbf{r}}^T \cdot \hat{\mathbf{K}}_0 \cdot \hat{\mathbf{r}}}. \tag{15}$$

Since $\hat{\mathbf{K}}_0$ is a positive definite matrix, the quadratic form in the denominator of (15) is a positive quantity. In contrast to $\hat{\mathbf{K}}_0$, $\dot{\hat{\mathbf{K}}}$ is an indefinite matrix, allowing, in principle, for positive, zero, and negative values of the quadratic form in the numerator of (15). The diagrammatic sketches in Fig. 3, inspired by numerical results obtained with the Abaqus displacement beam element B32OS [12], elucidate the meaning of the term *fundamental* eigenvalue. Fig. 2(a) refers to a problem with a stability limit in the form of a bifurcation point, denoted as S. In this case, the fundamental eigenvalue is the one for which $\hat{\chi}_1(\lambda_S) = 0$. Fig. 2(b) refers to a problem without a stability limit. In this case, the fundamental eigenvalue is the one that asymptotically tends to zero, *i.e.* $\lim_{\lambda\to\infty} \hat{\chi}_1(\lambda) = 0$. Obviously, this value has no physical significance. As follows from Fig. 3, the quadratic form in the numerator of (15) is a negative quantity.

None of the two diagrams in Fig. 3 contains a point of inflection. This is consistent with the assertion that it needs a linear eigenvalue problem of the kind of (4), based on hybrid elements, to obtain $\ddot{\chi}_1(\lambda) = 0$ ($(\Re(\chi_1))^{\cdot\cdot} = 0$) as the condition for the load level at maximum (minimum) stiffness of a proportionally loaded structure. The condition for a minimum value can obviously not be realized with the linear eigenvalue problem (11), because it does not allow that $\chi_1(\lambda)$ becomes a complex function. However, also the condition for a maximum value of the stiffness cannot be realized with this eigenvalue problem, which is solved with the

displacement elements that are the basis for their extension to the hybrid elements employed in this work. In the Appendix it will be shown that $\dot{\hat{\chi}}_1 = 0$ is restricted to the postbuckling region, whereas $\ddot{\chi}_1 = 0$ will be shown in Section 4 to occur in the prebuckling region.

In contrast to the monotonous decrease of $\hat{\chi}_1(\lambda)$ in Fig. 3(b), based on the said finite beam element, other displacement beam elements have resulted in non-monotonous relevant eigenvalue functions $\hat{\chi}_1(\lambda)$ for the same problem, see Fig. 11 in Kalliauer and Mang [1]. However, the extreme values of these eigenvalue functions are smaller than $1.0 \cdot 10^{-4}$, which hints at numerical artefacts. In contrast to the real eigenvalue functions $\hat{\chi}_1(\lambda)$, with positive curvatures, shown in Fig. 3, the corresponding eigenvalue functions $\chi_1(\lambda)$, not shown herein because of their qualitative similarity to the eigenvalue functions $\chi_1(\lambda)$ illustrated in Figs. 7 and 2, respectively, contain points of inflection, characterized by $\ddot{\chi}_1 = 0$ and $(\mathfrak{R}(\chi_1))^{\cdot\cdot} = 0$, respectively. The fact that, in the given case, the hybrid elements represent extensions of displacement elements corroborates the meaningfulness of the comparison of characteristics of corresponding eigenvalue curves (For the sake of simplification of the notation, the subscript 1 in the symbols for the fundamental eigenvalue, χ_1, and the corresponding eigenvector, $\mathbf{r}_1$, will generally be omitted.)

Since the Abaqus hybrid beam elements B32H and B32OSH are extensions of the Abaqus displacement beam elements B32 and B32OS, respectively, it is concluded that the quadratic forms

$$\mathbf{r}^T \cdot \dot{\mathbf{K}} \cdot \mathbf{r} \qquad \wedge \qquad \mathbf{r}^T \cdot \mathbf{K}_0 \cdot \mathbf{r} \tag{16}$$

in (14) have similar mathematical properties as the quadratic forms

$$\hat{\mathbf{r}}^T \cdot \dot{\hat{\mathbf{K}}} \cdot \hat{\mathbf{r}} \qquad \wedge \qquad \hat{\mathbf{r}}^T \cdot \hat{\mathbf{K}}_0 \cdot \hat{\mathbf{r}} \tag{17}$$

in (15). Hence, the bilinear forms

$$\mathbf{t}^T \cdot \dot{\mathbf{G}} \cdot \mathbf{r} \qquad \wedge \qquad \mathbf{t}^T \cdot \mathbf{G}_0 \cdot \mathbf{r} \tag{18}$$

in (14) represent a scientific added value of the hybrid beam elements. It consists in the mathematical possibility of physically motivated sign changes both in the numerator and the denominator of (14). The extreme values of the eigenvalue $\chi_1(\lambda)$ in Fig. 2(b) are characterized by the vanishing of the expression in the numerator of (14), *i.e.* by

$$\mathbf{r}^T \cdot \dot{\mathbf{K}} \cdot \mathbf{r} + 2\,\mathbf{t}^T \cdot \dot{\mathbf{G}} \cdot \mathbf{r} = 0. \tag{19}$$

The double eigenvalue $\chi_1(\lambda_L) = \chi_j(\lambda_L)$ and $\chi_1(\lambda_U) = \chi_j(\lambda_U)$ in Fig. 2(b) at the beginning and the end, respectively, of the region inside of which $\chi_1(\lambda)$ and $\chi_j(\lambda)$ are conjugate complex eigenvalues, is characterized by the vanishing of the expression in the denominator of (14), *i.e.* by

$$\mathbf{r}^T \cdot \mathbf{K}_0 \cdot \mathbf{r} + 2\,\mathbf{t}^T \cdot \mathbf{G}_0 \cdot \mathbf{r} = 0. \tag{20}$$

As mentioned in the Introduction, the value of λ at the point of inflection, I, see Fig. 2(b), of the function $\mathfrak{R}(\chi_1(\lambda)) = \mathfrak{R}(\chi_j(\lambda))$ is the load level at which the stiffness of the bar, subjected to eccentric compression, attains a minimum value. According to Fig. 2(b), this point is characterized by

$$(\mathfrak{R}(\chi_1(\lambda)))^{\cdot\cdot} = 0 \,. \tag{21}$$

In Section 4 it will be shown numerically that the condition for a maximum value of the stiffness of proportionally loaded structures is markedly different from the one for a minimum value.

Maximum and minimum values of the stiffness of such structures are impossible if

$$\frac{U_{\mathbf{M}}}{U} = \text{const.}. \tag{22}$$

This statement was verified numerically by checking the relevant eigenvalue function $\chi_1(\lambda)$ for the limiting cases of (22), *i.e.* for *pure stretching* and *pure bending*. (There are no other cases for which $U_{\mathbf{M}}/U = \text{const.}$.) Both functions were found to be monotonously decreasing from $\chi_1(\lambda = 0) = 1$ to $\chi_1(\lambda = \lambda_S) = 0$, without points of inflection. With the exception of the very moderately curved eigenvalue function for the limiting case of *pure bending*, obtained with displacement elements, all fundamental eigenvalue functions for both limiting cases were practically linear. Based on the disintegration of the first one of the two vector equations in (4), it can be shown that for these cases,

$$\mathbf{t}^T \cdot \dot{\mathbf{G}} \cdot \mathbf{r} = 0 \qquad \wedge \qquad \mathbf{t}^T \cdot \mathbf{G}_0 \cdot \mathbf{r} = 0, \tag{23}$$

which precludes (19) and (20). Substitution of (23) into (14) gives

$$\dot{\chi} = \frac{\mathbf{r}^T \cdot \dot{\mathbf{K}} \cdot \mathbf{r}}{\mathbf{r}^T \cdot \mathbf{K}_0 \cdot \mathbf{r}}, \tag{24}$$

which is of the same form as the expression for $\dot{\hat{\chi}}$, see (15), obtained with displacement elements.

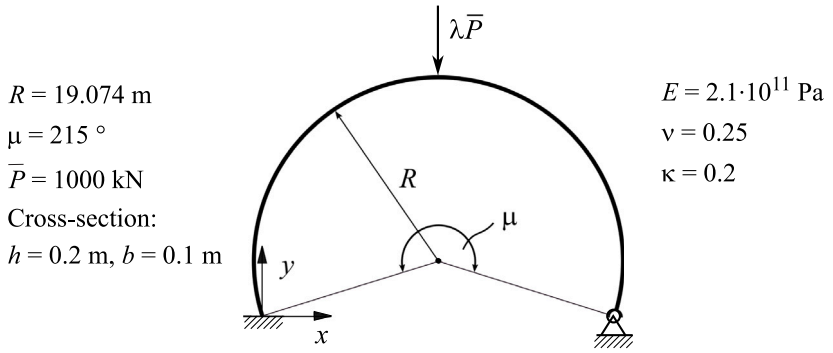

Fig. 4. Segment of a circular arch, clamped at one end and hinged at the other one, subjected to a vertical point load at its apex.

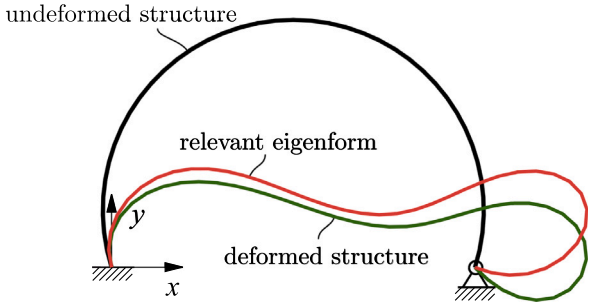

Fig. 5. Segment of a circular arch, clamped at one end and hinged at the other one, subjected to a vertical point load at its apex: deformed structure without superelevation and superimposed fundamental eigenform close before loss of stability by snap-through, obtained with Abaqus beam elements B32.

4. Numerical investigation

Fig. 4 shows a segment of a circular arch with the radius R and the read angle μ, clamped at one end and hinged at the other one. It is subjected to a quasi-static vertical point load, $\lambda\overline{P}$, at the apex of the arch segment; $\overline{P}$ denotes the reference load. The values of R, μ, and $\overline{P}$ are given as 19.074 m, 215°, and 1000 kN, respectively. The arch segment has a rectangular cross-section. Its height, h, is 0.2 m, and its width, b, is 0.1 m. The modulus of elasticity, E, Poisson's ratio, ν, and the shear coefficient, κ, are given as $2.1 \cdot 10^{11}$ Pa, 0.25, and 0.2, respectively.

The same structure was originally analyzed by Da Deppo and Schmidt [5]. It was re-analyzed *e.g.* by Pavlicek [6] and Helnwein [10]. At the times of these analyses, the search for conditions for extreme values of the stiffness of proportionally loaded structures had yet not been a topic of fundamental research in computational mechanics of structures. Nevertheless, the results of structural analyses of the arch by these authors have proved to be useful for the present research. The analyses by Pavlicek [6] and Helnwein [10] were performed with element #98 of the commercial finite element program MSC.MARC [13]. They are based on the so-called "Consistently Linearized Eigenvalue Problem" (CLE), which was originally proposed by Helnwein [10]. The CLE is defined as follows:

$$\left[\mathbf{K} + (\chi^{\circ} - \lambda)\dot{\mathbf{K}}\right] \cdot \mathbf{r}^{\circ} = \mathbf{0}. \tag{25}$$

In the prebuckling region, $\mathbf{K}$ is a positive-definite matrix. Consequently, the CLE would have been unsuitable for determination of the load level at minimum stiffness of the bar subjected to an eccentric compressive force, see Fig. 2(a), located in the complex region of the eigenvalue functions $\chi_1(\lambda)$ and $\chi_j(\lambda)$, see Fig. 2(b). Nevertheless, the coefficients of the characteristic polynomial of (25) can be made dimensionless. This is a necessary condition for at least qualitatively acceptable eigenvalue functions for problems with a maximum value of the stiffness.

Fig. 5 shows the deformed arch and the fundamental eigenform close before loss of stability of the structure by snap-through. The main reason for having chosen this example is the anticipated existence of a maximum value of the stiffness of the proportionally loaded arch before its decrease to zero at loss of stability by snap-through. The numerical investigation was carried out with Abaqus displacement elements B32 and Abaqus hybrid elements B32H. A convergence study has shown that the discretization of the arch segment with 40 elements provides sufficiently accurate results.

Fig. 6 shows $\lambda/\lambda_S - u$ and $\lambda/\lambda_S - \phi$ diagrams for (a) the apex of the arch ($x = 18.19$ m, $y = 24.81$ m) and (b) for a point close to its hinged support ($x = 36.84$ m, $y = 1.73$ m). u denotes the horizontal displacement of the arch and ϕ stands for the rotation of the tangent to its axis. At the stability limit, *i.e.* for $\lambda/\lambda_S = 1$, the curves have a horizontal tangent. The existence of points of inflection

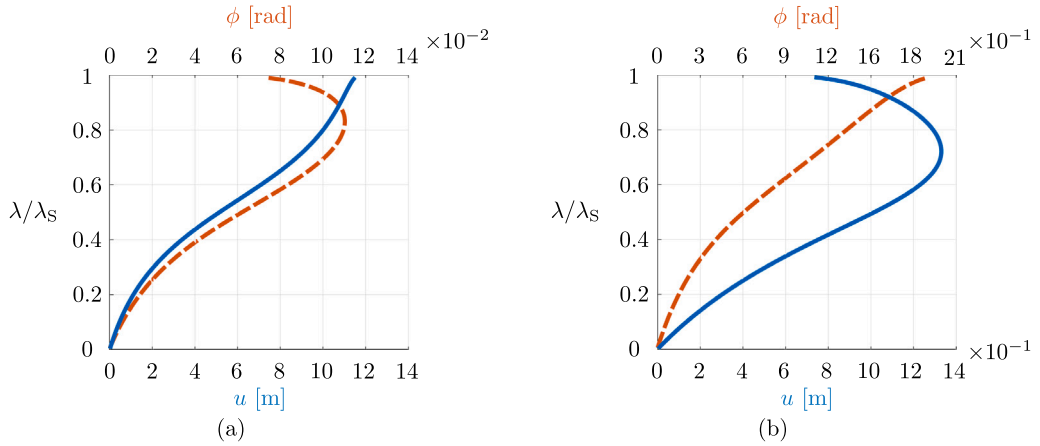

Fig. 6. Segment of a circular arch, clamped at one end and hinged at the other one, subjected to a vertical point load at its apex: $\lambda/\lambda_S - u$ diagram (solid blue curve) and $\lambda/\lambda_S - \phi$ diagram (dashed orange curve) for (a) $x = 18.19$ m, $y = 24.81$ m and (b) $x = 36.84$ m, $y = 1.73$ m, obtained with Abaqus hybrid beam elements B32H. (For interpretation of the references to colour in this figure legend, the reader is referred to the web version of this article.)

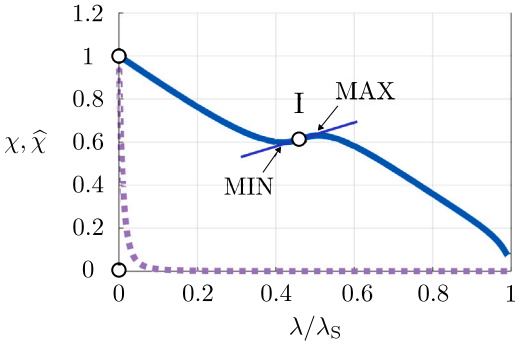

Fig. 7. Segment of a circular arch, clamped at one end and hinged at the other one, subjected to a vertical point load at its apex: $\chi - \lambda/\lambda_S$ diagram obtained with Abaqus hybrid elements B32H, see the solid curve, and $\widehat{\chi} - \lambda/\lambda_S$ diagram obtained with Abaqus displacement elements B32, see the dotted curve.

of the two diagrams in Fig. 6 is consistent with the comment of Helnwein [10] that all d.o.f.s of the apex of this structure contain such points. Helnwein's observation that the $\lambda/\lambda_S - u$ diagrams contain two points of inflection whereas the $\lambda/\lambda_S - \phi$ diagrams contain only one such point is confirmed by the diagrams in Fig. 6(a). The diagrams in Fig. 6(b), however, illustrate the opposite situation. This proves that the qualification of a proportionally loaded structure as *stiffening* or *softening* at the load level concerned on the basis of individual d.o.f.s is, in general, problematic.

Fig. 7 shows the $\chi - \lambda/\lambda_S$ diagram obtained with Abaqus B32H elements, see the solid curve, and the $\widehat{\chi} - \lambda/\lambda_S$ diagram obtained with Abaqus B32 elements, see the dotted curve. The snap-through point is a singular point, characterized by

$$\chi = 0, \quad \chi' = 0, \quad \lambda' = 0, \tag{26}$$

where $' := d/ds$ denotes an infinitesimal increment of the arc length of the curve. Thus,

$$\frac{d\chi}{d\lambda} = \frac{\chi'}{\lambda'} = \frac{0}{0} = \frac{\chi''}{\lambda''} < 0. \tag{27}$$

(The value of λ_S was extrapolated from the closest reliable numerical result for $\chi(\lambda/\lambda_S)$.) The $\chi - \lambda/\lambda_S$ diagram contains a point of inflection, I, located between a minimum value and a maximum value of the eigenvalue function $\chi(\lambda/\lambda_S)$. (*Nota bene*, such extreme values need not exist.) Point I signals a maximum value of the stiffness. In other words, the arch which has before been a stiffening structure becomes a softening structure. Point I is a consequence of points of inflection of individual d.o.f.s of the structure, occurring at different load levels, see Fig. 6. It is characterized by

$$\ddot{\chi}_1(\lambda) = 0 \quad , \tag{28}$$

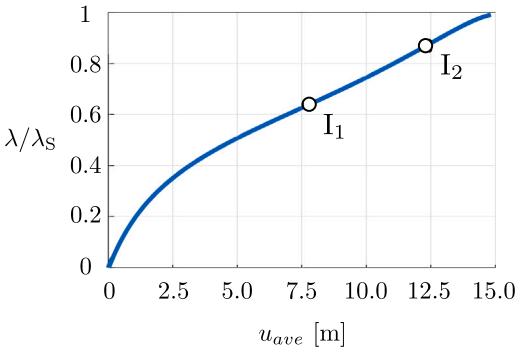

Fig. 8. Segment of a circular arch, clamped at one end and hinged at the other one, subjected to a vertical point load at its apex: $\lambda/\lambda_S - u_{ave}$ diagram, obtained with Abaqus hybrid beam elements B32H.

which is the key result of this work. It expresses the remarkable ability of the linear eigenvalue problem (4), the coefficient matrices of which are established with the help of hybrid finite elements, to determine the load level at the transition of the arch from a stiffening to a softening structure. Fig. 7 also shows that the linear eigenvalue problem (11), the coefficient matrices of which are established by means of displacement elements, is lacking this ability. *Nota bene*, apart from the stability limit, where $\chi(\lambda/\lambda_S) = \chi(1) = 0$, and the point of inflection, I, the eigenvalue function is mechanically insignificant.

A distinctive feature of the fundamental eigenvalue $\chi = \chi_1$ from five additionally computed eigenvalues of (4), not shown herein, is the absence of an imaginary part of χ_1. The condition for a maximum value of the stiffness of the investigated arch, see (28), differs markedly from the one for a minimum value of the stiffness of the bar subjected to eccentric compression, see (21). The latter refers to a structure without a stability limit. This forces the fundamental eigenvalue function to evade the abscissa of the $\chi - \lambda/\lambda_S$ system of reference on its way, starting at $\chi(\lambda = 0) = 1$, to negative values of χ. In contrast to the $\chi - \lambda/\lambda_S$ diagram, shown in Fig. 7, none of the previously investigated structures without an extreme value of the stiffness resulted in a non-monotonous $\chi - \lambda/\lambda_S$ diagram with a point of inflection, see *e.g.* Fig. 3 in [2].

The $\chi - \lambda/\lambda_S$ diagram obtained by Helnwein [10] is qualitatively similar to the one shown Fig. 7. Both diagrams start with a positive curvature and end with a negative curvature. The value of λ at the point of inflection in Helnwein's diagram, however, does not agree with the one in this paper. However, the CLE, used by Helnwein, has several deficiencies, among them the previously mentioned inability to produce conjugate complex eigenvalues in the prebuckling region. While the initial values of $\chi^\circ(\lambda)$ may be positive or negative, all initial values of $\chi(\lambda)$ are equal to 1. For the given problem, $\chi(\lambda)$ is a real function at least for $0 \le \lambda \le \lambda_S$. In contrast to the CLE, $\chi_i(\lambda) > 0$, $i = \{1, 2, \dots n\}$, for $0 \le \lambda < \lambda_S$.

Contrary to the function $\chi(\lambda/\lambda_S)$ in Fig. 7, the function $\hat{\chi}(\lambda/\lambda_S)$ in this figure is monotonously decreasing, without a point of inflection. Hence, displacement elements, resulting in two positive-definite coefficient matrices in the prebuckling region, see (11), are unsuitable for determination of extreme values of the stiffness of proportionally loaded structures.

In [1], an alternative condition for extreme values of the stiffness of proportionally loaded structures was presented. It reads as

$$\frac{d^2\xi}{d\lambda^2} = 0, \tag{29}$$

where

$$\xi = \frac{u_{ave}}{\int ds}, \tag{30}$$

is a dimensionless arc length. The "average displacement", u_{ave}, is defined as

$$u_{ave} = \frac{\int \|\mathbf{u}^*\| ds}{\int ds}, \tag{31}$$

where $\|\mathbf{u}^*\|$ denotes the Euclidean norm of the translational d.o.f.s of the structure and ds stands for an infinitesimal element of its axis. The aforementioned condition was used in [2] for determination of the load level at which the stiffness of a proportionally loaded bar subjected to eccentric compression, see Fig. 2(a), attains a minimum value. The result obtained for this load level agreed well with the one obtained with the condition $(\Re(\chi_1))^{\cdot\cdot} = (\Re(\chi_j))^{\cdot\cdot} = 0$, see Fig. 2(b).

Fig. 8 shows the $\lambda - u_{ave}$ diagram obtained for the arch investigated in this paper. Qualitatively, this diagram is similar to the $\lambda/\lambda_S - u$ diagram in Fig. 6(a) and the $\lambda/\lambda_S - \phi$ diagram in Fig. 6(b). Both diagrams contain two points of inflection. The second one is close to the snap-through point. However, the $\lambda/\lambda_S - u$ diagram in Fig. 6(b) and the $\lambda/\lambda_S - \phi$ diagram in Fig. 6(a) differ significantly from the $\lambda/\lambda_S - u_{ave}$ diagram, see Fig. 8. In view of the extremely large deformations of the arch it is not astonishing that a criterion which is based on an Euclidean norm and, thus, can only consider the translational d.o.f.s yields results for the load levels at which $(u_{ave})^{\cdot\cdot} = 0$, see points I_1 and I_2 in Fig. 8, that deviate significantly from the result for λ/λ_S at which $\ddot{\chi} = 0$, see point I in Fig. 7. In contrast to (31), the underlying linear eigenvalue problem considers all d.o.f.s. As mentioned previously, the coefficients of its characteristic polynomial can be made dimensionless. This is a necessary condition for physically meaningful results. Noting that

the investigated arch is obviously softening before snap-through, the existence of a load level at which the stiffness of the structure becomes a maximum value, well in advance of the stability limit rather than very close to it, is considered to be a plausible result.

5. Conclusions

Proportionally loaded structures, which are initially stiffening (softening), may turn into softening (stiffening) structures. At the load level of such a change the stiffness of the structure attains an extreme value. It was demonstrated numerically that this is a "global mechanical event" rather than one of a representative d.o.f. Determination of the load level at which it occurs was shown to require a "global mathematical tool" in the form of a special linear eigenvalue problem with two indefinite coefficient matrices. This allows for eigenvalue functions with regions inside of which they become complex functions. In contrast to the previously reported condition for the load level at which the stiffness of a proportionally loaded structure becomes a minimum, given as $(\Re(\chi_1(\lambda)))^{\cdot\cdot} = 0$, the respective condition for a maximum, presented in this work, was found to be $\ddot{\chi}_1(\lambda) = 0$. The reason for this fundamental difference is that a maximum value of the stiffness signals the beginning of the structure's tendency towards loss of stability, characterized by $\chi_1(\lambda_S) = 0$. Hence, in contrast to a minimum value of the stiffness, there is no need for a complex region of the eigenvalue function in order to postpone the possibility of an intersection of $\chi_1(\lambda)$ with the abscissa of the $\chi_1 - \lambda$ system of reference to a higher load level.

In order to underline the necessity of a linear eigenvalue problem with two indefinite coefficient matrices, established with Abaqus hybrid finite elements, the investigated structure was also analyzed with those Abaqus displacement elements that are the basis for their extension to the employed hybrid elements. However, the respective linear eigenvalue problem does not have two indefinite coefficient matrices. Hence, the condition for the load level at which the stiffness attains a minimum value cannot be realized. However, also the condition for the load level at which the stiffness of a structure becomes a maximum cannot be realized, because the real eigenvalue function concerned does not have a point of inflection in the prebuckling region, as was shown in the Appendix. Moreover, this load level can also not be determined in the form of a point of inflection of a representative d.o.f.. Its computation is based on the Euclidean norm of the translational d.o.f.s. While the unavoidable disregard of the rotational d.o.f.s is insignificant in case of the example of a bar subjected to an eccentric compressive force, this does not apply to the example of a segment of a circular arch, subjected to a point load at its apex.

The nucleus of the conclusions reads as follows: The linear eigenvalue problem (11), with the tangent stiffness matrix and the small-displacement stiffness matrix as the two coefficient matrices, imposes constraints on the eigenvalue functions. Hybrid elements in the form of an extension of displacement elements, resulting in the linear eigenvalue problem (4), enable the removal of those constraints that prevent the determination of the load level at which the stiffness of a proportionally loaded structure attains an extreme value.

It would be astonishing if a linear eigenvalue problem with an amazing mechanical potential at the "eigenvalue level" had no comparatively surprising mechanical potential at the "eigenvector level". Indeed, the assumed correlation of points of inflection at the "eigenvalue level" with points of inflection at the "eigenvector level", is an example for the great potential of this eigenvalue problem at both levels. An interesting question for further research is whether or not an extreme value of $U_{\mathbf{M}}/U$ is necessarily preceded by an extreme value of the stiffness of the structure. To answer this question requires the numerical verification of the mentioned correlation. This is beyond the scope of this work, which is restricted to the determination of eigenvalue functions with special mechanical properties. Another interesting research question is whether or not $U_{\mathbf{M}}/U$ is equal to the radius of curvature of a curve, described by the vertex of a unit vector resulting from normalization of a modification of the fundamental eigenvector of the linear eigenvalue problem used in this work. A challenge of this modification is the requirement that the components of this vector are dimensionless quantities. An example with three d.o.f.s for this modification was presented in Section 2.

CRediT authorship contribution statement

A. Wagner: Visualization, Validation, Software, Investigation, Formal analysis, Data curation. **J. Kalliauer:** Visualization, Validation, Software, Investigation, Formal analysis, Data curation. **M. Aminbaghai:** Writing – review & editing, Writing – original draft, Visualization, Validation. **H.A. Mang:** Writing – review & editing, Writing – original draft, Supervision, Resources, Project administration, Methodology, Investigation, Funding acquisition, Formal analysis, Conceptualization.

Declaration of competing interest

The authors declare that they have no known competing financial interests or personal relationships that could have appeared to influence the work reported in this paper.

Data availability

Data will be made available on request.

Acknowledgements

A. Wagner wishes to acknowledge financial support by the Austrian Science Fund (FWF) in the framework of the research project P 31617-N32 [Pseudo-kinematic invariants - gems in FE structural analyses], sponsored by the FWF.

Appendix. Proof that $\ddot{\hat{\chi}}_1 \equiv \ddot{\hat{\chi}} = 0$, resulting from the linear eigenvalue problem (11), can only occur in the postbuckling region

Derivation of (13) with respect to λ gives

$$\left[\ddot{\hat{\mathbf{K}}} - \ddot{\hat{\chi}}\hat{\mathbf{K}}_0\right] \cdot \hat{\mathbf{r}} + 2\left[\dot{\hat{\mathbf{K}}} - \dot{\hat{\chi}}\hat{\mathbf{K}}_0\right] \cdot \dot{\hat{\mathbf{r}}} + \left[\hat{\mathbf{K}} - \hat{\chi}\hat{\mathbf{K}}_0\right] \cdot \ddot{\hat{\mathbf{r}}} = \mathbf{0}. \tag{A.1}$$

Premultiplication of (A.1) by $\hat{\mathbf{r}}^T$ and consideration of (11) yields

$$\hat{\mathbf{r}}^T \cdot \left[\ddot{\hat{\mathbf{K}}} - \ddot{\hat{\chi}}\hat{\mathbf{K}}_0\right] \cdot \hat{\mathbf{r}} + 2\hat{\mathbf{r}}^T \cdot \left[\dot{\hat{\mathbf{K}}} - \dot{\hat{\chi}}\hat{\mathbf{K}}_0\right] \cdot \dot{\hat{\mathbf{r}}} = 0. \tag{A.2}$$

Premultiplication of (13) by $\dot{\hat{\mathbf{r}}}^T$ results in

$$\dot{\hat{\mathbf{r}}}^T \cdot \left[\dot{\hat{\mathbf{K}}} - \dot{\hat{\chi}}\hat{\mathbf{K}}_0\right] \cdot \hat{\mathbf{r}} + \dot{\hat{\mathbf{r}}}^T \cdot \left[\hat{\mathbf{K}} - \hat{\chi}\hat{\mathbf{K}}_0\right] \cdot \dot{\hat{\mathbf{r}}} = 0, \tag{A.3}$$

Substitution of (A.3) into (A.2) gives

$$\hat{\mathbf{r}}^T \cdot \left[\ddot{\hat{\mathbf{K}}} - \ddot{\hat{\chi}}\hat{\mathbf{K}}_0\right] \cdot \hat{\mathbf{r}} - 2\dot{\hat{\mathbf{r}}}^T \cdot \left[\hat{\mathbf{K}} - \hat{\chi}\hat{\mathbf{K}}_0\right] \cdot \dot{\hat{\mathbf{r}}} = 0. \tag{A.4}$$

In the following, the assumption that

$$\ddot{\hat{\chi}} = 0 \tag{A.5}$$

correlates with

$$\dot{\hat{\mathbf{r}}}^T \cdot \hat{\mathbf{K}} \cdot \dot{\hat{\mathbf{r}}} = 0 \tag{A.6}$$

will be verified. The vanishing of this quadratic form requires that $\hat{\mathbf{K}}$ is an indefinite matrix. This is the case in the postbuckling region, $\lambda > \lambda_S$, where

$$\hat{\chi} < 0. \tag{A.7}$$

Substitution of (A.5) and (A.6) into (A.4) gives

$$\hat{\chi}\Big|_{\ddot{\hat{\chi}}=0} = -\frac{\hat{\mathbf{r}}^T \cdot \ddot{\hat{\mathbf{K}}} \cdot \hat{\mathbf{r}}}{2\dot{\hat{\mathbf{r}}}^T \cdot \hat{\mathbf{K}}_0 \cdot \dot{\hat{\mathbf{r}}}} < 0. \tag{A.8}$$

Since $\hat{\mathbf{K}}_0$ is a positive-definite matrix,

$$\dot{\hat{\mathbf{r}}}^T \cdot \hat{\mathbf{K}}_0 \cdot \dot{\hat{\mathbf{r}}} > 0. \tag{A.9}$$

To check whether

$$\hat{\mathbf{r}}^T \cdot \ddot{\hat{\mathbf{K}}} \cdot \hat{\mathbf{r}}\Big|_{\ddot{\hat{\chi}}=0} > 0, \tag{A.10}$$

as must be in the case if (A.8) is correct, (A.4) is investigated. Noting that $\hat{\mathbf{K}} - \hat{\chi}\hat{\mathbf{K}}_0$ is a positive-semidefinite matrix which is singular and that $\dot{\hat{\mathbf{r}}}$ is not an eigenvector of this matrix,

$$\dot{\hat{\mathbf{r}}}^T \cdot \left[\hat{\mathbf{K}} - \hat{\chi}\hat{\mathbf{K}}_0\right] \cdot \dot{\hat{\mathbf{r}}} > 0. \tag{A.11}$$

As follows from (A.4) and (A.11),

$$\hat{\mathbf{r}}^T \cdot \left[\ddot{\hat{\mathbf{K}}} - \ddot{\hat{\chi}}\hat{\mathbf{K}}_0\right] \cdot \hat{\mathbf{r}} > 0. \tag{A.12}$$

Specialization of (A.12) for $\ddot{\hat{\chi}} = 0$ results in (A.10). Thus, (A.8), which rests on the correlation of (A.5) with (A.6), is verified. In the prebuckling region, $0 < \hat{\chi}(\lambda) \leq 1$. At the stability limit, $\hat{\chi}(\lambda_S) = 0$. Hence, $\ddot{\hat{\chi}} = 0$ can only occur in the postbuckling region, *quod erat demonstrandum*.

References

[1] J. Kalliauer, H.A. Mang, Are the terms *stiffening/softening structures* mechanically unambiguous? Eur. J. Mech. A Solids 96 (2022) 104756, http://dx.doi.org/10.1016/j.euromechsol.2022.104756.

[2] J. Kalliauer, H.A. Mang, Conditions for minimum stiffness of proportionally loaded structures, Comput. Methods Appl. Mech. Engrg. 404 (2023) 115820, https://gitlab.imws.tuwien.ac.at/jkalliau/MangAbaqus.

[3] J. Kalliauer, M. Malendowski, H.A. Mang, On a remarkable geometric-mechanical synergism based on a novel linear eigenvalue problem, Acta Mech. 232 (2021) 4969–4985, http://dx.doi.org/10.1007/s00707-021-03091-5.

[4] C.R. Wylie, Advanced engineering mathematics, Sixth ed., McGraw-Hill, New York, 1995.

[5] D.A. Da Deppo, R. Schmidt, Instability of clamped-hinged circular arches, subjected to point load, Am. Soc. Mech. Eng. (1975) 894–896.

[6] S. Pavlicek, Die Beulkugel: Eine Symbiose von Mechanik und Geometrie [in German: The Buckling Sphere: A Symbiosis of Mechanics and Geometry] (Ph.D. thesis), Vienna University of Technology [now TU Wien], Wien, 2016.

[7] P. Wriggers, J.C. Simo, A general procedure for the direct computation of turning and bifurcation points, Internat. J. Numer. Methods Engrg. 30 (1) (1990) 155–176.
[8] B. Brendel, Geometrisch nichtlineare Elastostatik [in German: Geometrically nonlinear elastostatics] (Ph.D. thesis), Institute for Structural Mechanics, University of Stuttgart, Stuttgart, Germany, 1979.
[9] V. Theofilis, Advances in global linear instability analysis of nonparallel and three-dimensional flows, Prog. Aerosp. Sci. 39 (4) (2003) 249–315.
[10] P. Helnwein, Zur initialen Abschätzbarkeit von Stabilitätsgrenzen auf nichtlinearen Last-Verschiebungspfaden elastischer Strukturen mittels der Methode der Finiten Elemente [in German: On *ab initio* accessability of stability limits on nonlinear load-displacment paths of elastic structures by means of the finite element method] (Ph.D. thesis), Vienna University of Technology [now TU Wien], Vienna, Austria, 1996, URL: https://permalink.catalogplus.tuwien.at/AC02254015.
[11] R.H. Gallagher, H.T. Yang, Elastic instability predictions for doubly curved shells, in: Proceedings of the 2nd Conference on Matrix Methods in Structural Mechanics, Wright-Patterson A.F. Base, 1968, pp. 711–739.
[12] Abaqus User Manual, Abaqus 2021 Theory Guide, Dassault Systemes Simulia Corp., 2020.
[13] Marc Manual, Theory and User Information Guide, MSC Software Corp., 2012.